



LAWRENCE
LIVERMORE
NATIONAL
LABORATORY

Synthesis of ZnO coated Activated Carbon Aerogel by Simple Sol-Gel Route

T. Y. Han, M. A. Worsley, T. F. Baumann, J. H.
Satcher Jr.

September 27, 2010

Journal of Materials Chemistry

Disclaimer

This document was prepared as an account of work sponsored by an agency of the United States government. Neither the United States government nor Lawrence Livermore National Security, LLC, nor any of their employees makes any warranty, expressed or implied, or assumes any legal liability or responsibility for the accuracy, completeness, or usefulness of any information, apparatus, product, or process disclosed, or represents that its use would not infringe privately owned rights. Reference herein to any specific commercial product, process, or service by trade name, trademark, manufacturer, or otherwise does not necessarily constitute or imply its endorsement, recommendation, or favoring by the United States government or Lawrence Livermore National Security, LLC. The views and opinions of authors expressed herein do not necessarily state or reflect those of the United States government or Lawrence Livermore National Security, LLC, and shall not be used for advertising or product endorsement purposes.

Synthesis of ZnO coated Activated Carbon Aerogel

by Simple Sol-Gel Route

T. Yong-Jin Han*, Marcus A. Worsley, Theodore F. Baumann, Joe H. Satcher Jr.

Physical and Life Sciences Directorate

Lawrence Livermore National Laboratory

Livermore, CA 94550

Received Date (inserted by publisher)

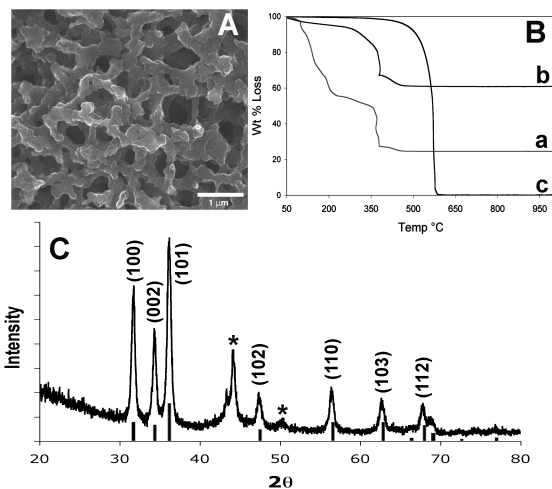
Revised Received Date (inserted by publisher)

Porous materials with high surface area have shown promise in fuel cells,¹ catalysis,² photovoltaic³ and sensor applications.⁴ These high surface area materials can be synthesized using sol-gel chemistry,⁵ soft templating⁶ and hard templating approaches.⁷ Although many useful semiconductors have been obtained by these methods, synthesis of high surface area zinc oxide (ZnO) has been somewhat limited. Zinc oxide (ZnO) is an important II-IV, n-type semiconductor material with a wide band gap of $\Delta E_{\text{gap}} = 3.37$ eV with an exciton-binding energy of 60 meV. It also possesses interesting optical properties (i.e. transparent conducting film) as well as piezoelectric properties.⁸ These novel properties of ZnO have led to applications in catalysis,⁹ UV-light emitting diodes,¹⁰ lasers,¹¹ gas¹² and bio-sensors.¹³ Another interesting application of ZnO is its use in photovoltaic solar cells. Previously Cao et al.¹⁴ and Yang et al.¹⁵ have successfully utilized aggregated nanocrystallites and nanowires of ZnO respectively, to fabricate efficient dye-sensitized solar cells (DSC). Although these examples proved the usefulness of ZnO in such application, the low surface areas in both systems limited the conversion efficiency of solar energy to electrical energy.

Numerous attempts at achieving high surface area ZnO have been made, including surfactant templated methods. Although surfactant driven synthesis of ZnO has been successful in synthesizing nanostructured ZnO, the internal surface areas were not accessible due to the presence of the structure directing agents.¹⁶ Other examples of high surface area ZnO were achieved by sol-gel processing¹⁷ and hard templating methods.¹⁸ As a hard template material for ZnO, activated carbon aerogels (ACAs) show a great potential due to their high surface area ($1000\text{-}3000\text{ m}^2\text{ g}^{-1}$), thermal stability, mechanical robustness and high electrical conductivity.¹⁹ Therefore, having ACAs as the underlying structure coated with ZnO will not only produce high surface

area ZnO, but may yield improved electron transfer property. Herein, we report the synthesis of high surface area ZnO-carbon composite using ACAs as templates for the deposition of ZnO using sol-gel chemistry.

The ACAs are prepared through carbonization and thermal activation of organic aerogels derived from resorcinol and formaldehyde, as previously described.¹⁹ As seen from Figure 1A, the microstructure of the ACA template is composed of interconnected sub-micron-sized carbon particles that define a continuous macroporous network. The high surface area of the ACA arise from the micro- and small mesopores formed within the carbon particles during thermal activation. One of the key aspect of this structure is the continuous macropore network that allows for uniform infiltration of ZnO sol-gel solution throughout the ACA architecture. The ZnO sol-gel solution was prepared by addition of propylene oxide to a methanolic solution of zinc nitrate hexahydrate.¹⁷ In this reaction, propylene oxide acts as an acid scavenger, driving the formation of zinc hydroxide through hydrolysis and condensation of hydrated zinc ions. Monolithic ACA parts were then immersed in the sol-gel solution mixture under vacuum to allow for complete infiltration of the aerogel porosity. Evacuation of the system was continued to concentrate the sol-gel solution through evaporation of methanol and induce deposition of $\text{Zn}(\text{OH})_2$ on the internal surfaces of the template. Complete drying of the mixture under vacuum resulted in fully coated ACA composite material. It is important to mention that the use of methanol as the solvent for the sol-gel solution is essential for wetting



the carbon framework of ACA.

Figure 1. A) SEM micrograph of ACA taken with JOEL7401-F with SEI detector at 5 KV. B) TGA analysis of a) as-made ZnO-ACA, b) ZnO-ACA thermally treated at 250 °C and c) pure ACA, performed with Shimadzu TGA-50 with flowing air at 20 sccm/min with heating rate of 10 °C/min. C) X-ray diffraction pattern of ZnO-ACA thermally treated at 250 °C taken with Scintag PAD-V X-ray diffractometer with Cu K α radiation at 40 kV and 30 mA. * denotes peaks from carbon.

The thermogravimetric analysis (TGA) of as-prepared composite material (Fig. 1B-a) shows multiple events occurring from room temperature (r.t.) to 450 °C. The initial weight loss from r.t. to 100 °C can be attributed to the loss of adsorbed methanol and water, followed by dehydration and crystallization of different polymorphs of Zn(OH)₂. A variety of phases can potentially form from the hydrolysis and condensation of Zn(II) ions, including amorphous Zn(OH)₂, the α , δ , or ϵ phases,²⁰ as well as a salt adduct, Zn₅(OH)₈(NO₃)₂·2H₂O.²¹ For the propylene oxide induced sol-gel chemistry used to make the composite material, the expected phases of zinc hydroxide are the ϵ and the nitrate adduct. As shown in Figure 1B-a, annealing of the composite at 250 °C converts all of the deposited Zn(OH)₂ to ZnO as evidenced by no significant weight loss. The crystallinity of the ZnO on the ACA framework is confirmed by X-ray diffraction (XRD). The XRD diffraction pattern for the composite after thermal annealing at 250 °C (Fig. 1C) shows well-defined peaks that correlate with those expected for crystalline ZnO (zincite, PDF# 36-1451, hexagonal, a= 3.2498, c= 5.20661, P63mc, space group=186) with no trace of Zn(OH)₂ peaks.

The crystallinity of the deposited ZnO is also evident from SEM micrographs taken from a cross section of the annealed composite. As shown in Fig 2A, the surfaces of the ACA template are clearly coated with crystalline and well-faceted ZnO nanoparticles, and the coating appears to be uniform throughout the ACA framework. A higher resolution SEM image of the composite (Fig. 2A inset) shows that the coating is comprised of randomly oriented ZnO crystallites that are 10-50 nm in size. The intimate contact, apparent in the SEM images, between ZnO crystallites and the continuous carbon framework should yield favorable electron transport properties in these composite architectures. The uniformity of the ZnO coating within the ACA template was determined using energy dispersive X-ray spectroscopy mapping (EDS). As seen in Figure 2B, the EDS maps show that carbon, oxygen and zinc are uniformly distributed throughout the ZnO-ACA composite. This observation confirms that the sol-gel solution fully penetrated the internal porosity of the monolithic ACA template during infiltration. The ZnO content in this composite was determined by TGA to be 60 wt % (Fig. 1B-b). By decreasing the concentration of Zn(NO₃)₂ in the sol-gel reaction, we were also able to prepare composite materials with lower ZnO content. SEM analysis of a ZnO-ACA composite with 20 wt % ZnO showed that the surface looked very much like that of the starting template, suggesting that the ACA is coated with a very small crystallites of ZnO. Closer examination of the surface by TEM (Fig. 3A) shows that the template is indeed evenly coated by ZnO nanoparticles (diameters ~5 nm) that are significantly smaller than those seen in the 60 wt % composite.

The BET surface areas of the 60 and 20 wt % ZnO-ACA composites are 439 and 1515 m² g⁻¹ respectively. Both values are significantly lower than that measured for the

starting ACA (2600 m² g⁻¹). Since the intrinsic surface area of the ZnO crystallites is significantly lower than that of the ACA substrate, a decrease in gravimetric surface area would be expected following deposition of ZnO within the ACA, especially at these high loading levels. The fact that the surface areas of the composites decrease with increasing ZnO loading supports this contention. In addition, the ZnO coating likely plugs much of the micro- and small mesopores that populate the ACA framework, also leading to a drop in surface area. Nevertheless, the surface areas of these ZnO-ACA composites are significantly higher than those reported for other porous ZnO nanostructures.²²

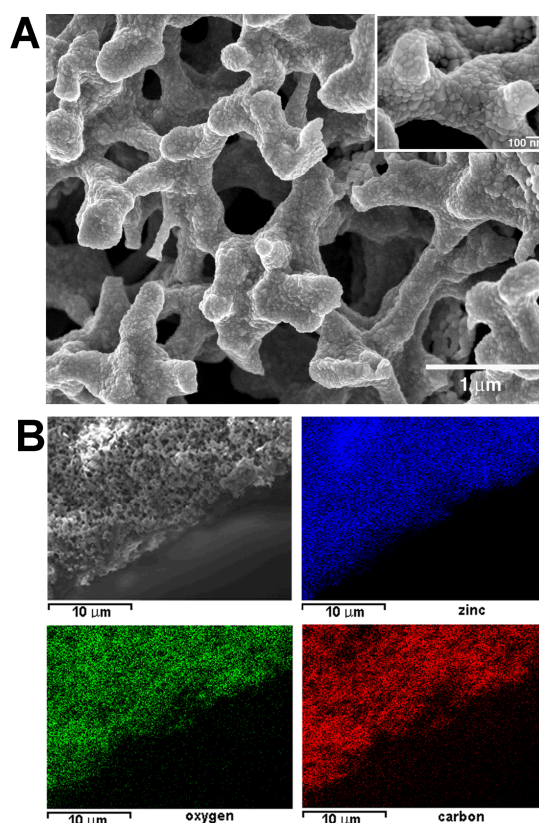


Figure 2. A) SEM micrograph of ZnO-ACA thermally treated at 250 °C with inset showing higher resolution micrograph. B) SEM and EDS analysis of ZnO-ACA (250°C) probing carbon, oxygen and zinc using Oxford Inca EDS system.

From the TGA data, we also observed rapid weight loss at ~380 °C (Fig. 1B-b) in these composites that can be attributed to oxidation and burn-off of the carbon template. While the uncoated ACA is typically stable up to ~600 °C (Fig. 1B-c), the presence of the ZnO nanoparticles apparently catalyzes carbon burn-off at lower temperatures. Based on this observation, we attempted to prepare pure ZnO replicate structures through thermal removal of the ACA template from these composites. Interestingly, after thermal annealing of 20 wt % loaded sample at 450 °C, the remaining ZnO replica retains the same general microstructure of the original ACA template (Figure 3B). Examination of the replicate structure by TEM shows that the ZnO nanoparticles ripen during template removal (Figure 3B-inset). Apparently, this ripening leads not only to larger crystallites (diameters ranging from 20-40 nm), but also

stronger connections between adjacent particles that allow the structure to hold together after the ACA template is removed. However, the amount of ZnO replica structure produced via thermal annealing process produced only a few milligrams per reaction, too small of an amount for BET analysis. Template removal from composites containing 60 wt % ZnO produced material with minimal porosity, likely due to ripening effects of larger ZnO nanoparticles during thermal annealing.

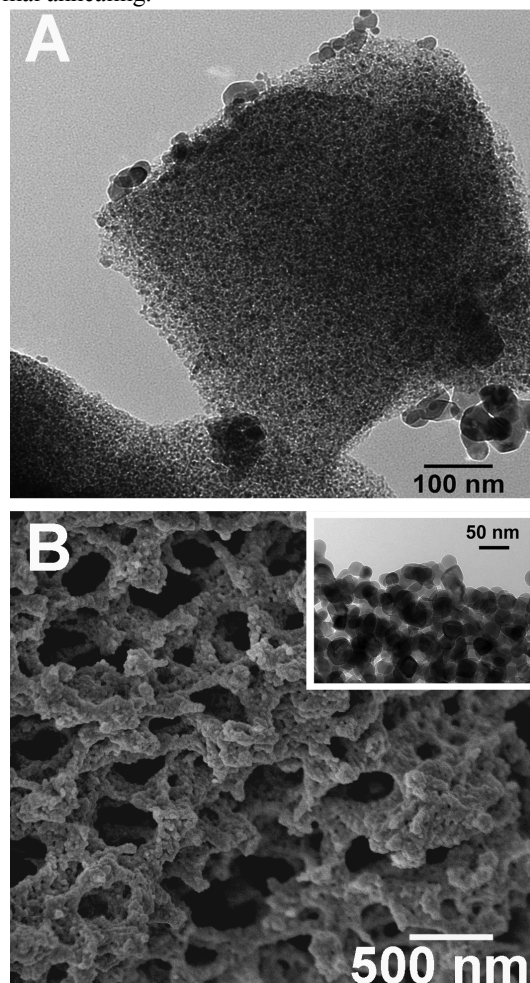


Figure 3. A) TEM analysis of ZnO-ACA (20 wt% loaded) sample showing uniform distribution of ZnO nanoparticles in a ACA particle. TEM measurements were made on a Philips FEG CM300, operating at 300 kV using copper grids with lacey formvar. B) SEM micrograph of ZnO-ACA after thermally removing carbon by heating the sample at 450 °C. Inset, TEM micrograph of B) showing ZnO nanoparticles (20-40 nm) without carbon framework.

In summary, we demonstrated the synthesis of novel ZnO-ACA composites that exhibit high surface areas and well-crystallized ZnO nanoparticles. These materials are prepared by coating Zn(OH)₂ particles using sol-gel chemistry on the internal porosity of high surface area ACA templates. The sol-gel coatings are uniform throughout the ACA structure. Thermal treatment of the as-prepared composite material resulted in the formation of well-faceted ZnO nanoparticles that completely cover the carbon framework. The surface areas of the ZnO-ACA composites can be controlled through the ZnO loading and can range from 1500 m² g⁻¹ (20 wt % ZnO loading) to 400 m² g⁻¹ (60 wt % ZnO loading). We also

demonstrate that the ACA can be removed thermally to yield ZnO nanostructures that retain the original porous network architecture of the template. The high surface area of ZnO-ACA composite materials, along with intimate contact between ZnO and the electrically-conductive carbon framework, make these materials viable candidates for a variety of applications. In addition, the synthetic approach presented here is general and can readily be applied to the fabrication of carbon composites with other semiconductors.

Acknowledgment This work performed under the auspices of the U.S. Department of Energy by Lawrence Livermore National Laboratory under Contract DE-AC52-07NA27344. The project 09-LW-024 was funded by the Laboratory Directed Research and Development Program at LLNL.

Supporting Information Available. Detailed Experimental Sections.

References

1. a)Teng, X. W.; Liang, X. Y.; Rahman, S.; Yang, H., *Adv. Mater.* **2005**, 17, (18), 2237-2241; b)Chai, G. S.; Yoon, S. B.; Yu, J. S.; Choi, J. H.; Sung, Y. E., *J. Phys. Chem. B* **2004**, 108, (22), 7074-7079; c)Hyeon, T.; Han, S.; Sung, Y. E.; Park, K. W.; Kim, Y. W., *Angew. Chem.-Int. Edit.* **2003**, 42, (36), 4352-4356; d)Mamak, M.; Coombs, N.; Ozin, G., *J. Am. Chem. Soc.* **2000**, 122, (37), 8932-8939.
2. a)Corma, A., *Chem. Rev.* **1997**, 97, (6), 2373-2419; b)Taguchi, A.; Schuth, F., *Microporous Mesoporous Mat.* **2005**, 77, (1), 1-45; c)Wu, C. D.; Hu, A.; Zhang, L.; Lin, W. B., *J. Am. Chem. Soc.* **2005**, 127, (25), 8940-8941.
3. a)Barbe, C. J.; Arendse, F.; Comte, P.; Jirousek, M.; Lenzmann, F.; Shklover, V.; Gratzel, M., *J. Am. Ceram. Soc.* **1997**, 80, (12), 3157-3171; b)Coakley, K. M.; McGehee, M. D., *Appl. Phys. Lett.* **2003**, 83, (16), 3380-3382.
4. a)Teoh, L. G.; Hon, Y. M.; Shieh, J.; Lai, W. H.; Hon, M. H., *Sens. Actuator B-Chem.* **2003**, 96, (1-2), 219-225; b)Cosnier, S.; Senillou, A.; Gratzel, M.; Comte, P.; Vlachopoulos, N.; Renault, N. J.; Martelet, C., *J. Electroanal. Chem.* **1999**, 469, (2), 176-181; c)Lee, D.; Lee, J.; Kim, J.; Na, H. B.; Kim, B.; Shin, C. H.; Kwak, J. H.; Dohnalkova, A.; Grate, J. W.; Hyeon, T.; Kim, H. S., *Adv. Mater.* **2005**, 17, (23), 2828-+.
5. Brinker, C. J.; Scherer, G. W., *Sol-Gel Science: The Physics and Chemistry of Sol-Gel Processing*. Academic Press: 1990.
6. a)Beck, J. S.; Vartuli, J. C.; Roth, W. J.; Leonowicz, M. E.; Kresge, C. T.; Schmitt, K. D.; Chu, C. T. W.; Olson, D. H.; Sheppard, E. W.; McCullen, S. B.; Higgins, J. B.; Schlenker, J. L., *J. Am. Chem. Soc.* **1992**, 114, (27), 10834-10843; b)Yang, P. D.; Zhao, D. Y.; Margolese, D. I.; Chmelka, B. F.; Stucky, G. D., *Chem. Mat.* **1999**, 11, (10), 2813-2826.
7. a)Rumplecker, A.; Kleitz, F.; Salabas, E. L.; Schuth, F., *Chem. Mat.* **2007**, 19, (3), 485-496; b)Ryoo, R.; Joo, S. H.; Jun, S., *J. Phys. Chem. B* **1999**, 103, (37), 7743-7746; c)Yang, H. F.; Shi, Q. H.; Liu, X. Y.; Xie, S. H.; Jiang, D. C.; Zhang, F. Q.; Yu, C. Z.; Tu, B.; Zhao, D. Y., *Chem. Commun.* **2002**, (23), 2842-2843; d)Gao, F.; Lu, Q. Y.; Zhao, D. Y., *Adv. Mater.* **2003**, 15, (9), 739-742.
8. a)Wang, Z. L., *J. Phys.-Condes. Matter* **2004**, 16, (25), R829-R858; b)Klingshirn, C., *Phys. Status Solidi B-Basic Solid State Phys.* **2007**, 244, (9), 3027-3073; c)Ozgur, U.; Alivov, Y. I.; Liu, C.; Teke, A.; Reschikov, M. A.; Dogan, S.; Avrutin, V.; Cho, S. J.; Morkoc, H., *J. Appl. Phys.* **2005**, 98, (4).
9. a)Sarvari, M. H.; Sharghi, H., *Tetrahedron* **2005**, 61, (46), 10903-10907; b)Pauporte, T.; Rathousky, J., *J. Phys. Chem. C* **2007**, 111, (21), 7639-7644; c)Chin, Y. H.; Dagle, R.; Hu, J. L.; Dohnalkova, A. C.; Wang, Y., *Catal. Today* **2002**, 77, (1-2), 79-88.
10. a)Tsukazaki, A.; Ohtomo, A.; Onuma, T.; Ohtani, M.; Makino, T.; Sumiya, M.; Ohtani, K.; Chichibu, S. F.; Fuke, S.; Segawa, Y.; Ohno, H.; Koizumi, H.; Kawasaki, M., *Nat. Mater.* **2005**, 4, (1), 42-46; b)Bao, J. M.; Zimmler, M. A.; Capasso, F.; Wang, X. W.; Ren, Z. F., *Nano Lett.* **2006**, 6, (8), 1719-1722.

11. Huang, M. H.; Mao, S.; Feick, H.; Yan, H. Q.; Wu, Y. Y.; Kind, H.; Weber, E.; Russo, R.; Yang, P. D., *Science* **2001**, 292, (5523), 1897-1899.
12. a) Wagner, T.; Waitz, T.; Roggenbuck, J.; Froba, M.; Kohl, C. D.; Tiemann, M., *Thin Solid Films* **2007**, 515, (23), 8360-8363; b) Ahn, M. W.; Park, K. S.; Heo, J. H.; Park, J. G.; Kim, D. W.; Choi, K. J.; Lee, J. H.; Hong, S. H., *Appl. Phys. Lett.* **2008**, 93, (26).
13. Wei, A.; Sun, X. W.; Wang, J. X.; Lei, Y.; Cai, X. P.; Li, C. M.; Dong, Z. L.; Huang, W., *Appl. Phys. Lett.* **2006**, 89, (12).
14. Zhang, Q. F.; Chou, T. R.; Russo, B.; Jenekhe, S. A.; Cao, G. Z., *Angew. Chem.-Int. Edit.* **2008**, 47, (13), 2402-2406.
15. Law, M.; Greene, L. E.; Johnson, J. C.; Saykally, R.; Yang, P. D., *Nat. Mater.* **2005**, 4, (6), 455-459.
16. a) Tan, Y. W.; Steinmiller, E. M. P.; Choi, K. S., *Langmuir* **2005**, 21, (21), 9618-9624; b) Choi, K. S.; Lichtenegger, H. C.; Stucky, G. D.; McFarland, E. W., *J. Am. Chem. Soc.* **2002**, 124, (42), 12402-12403.
17. Gao, Y. P.; Sisk, C. N.; Hope-Weeks, L. J., *Chem. Mat.* **2007**, 19, (24), 6007-6011.
18. Polarz, S.; Orlov, A. V.; Schuth, F.; Lu, A. H., *Chem.-Eur. J.* **2007**, 13, (2), 592-597.
19. Baumann, T. F.; Worsley, M. A.; Han, T. Y. J.; Satcher, J. H., *J. Non-Cryst. Solids* **2008**, 354, (29), 3513-3515.
20. a) Beverskog, B.; Puigdomenech, I., *Corros Sci* **1997**, 39, (1), 107-114; b) Shaporev, A. S.; Ivanov, V. K.; Baranchikov, A. E.; Polezhaeva, O. S.; Tret'yakov, Y. D., *Russ J Inorg Chem+* **2007**, 52, (12), 1811-1816.
21. Meyn, M.; Beneke, K.; Lagaly, G., *Inorg Chem* **1993**, 32, (7), 1209-1215.
22. a) Carnes, C. L.; Klabunde, K. J., *Langmuir* **2000**, 16, (8), 3764-3772; b) Chandra, D.; Mridha, S.; Basak, D.; Bhaumik, A., *Chem. Commun.* **2009**, (17), 2384-2386.

Table of Contents Graphic and Summary

T. Yong-Jin Han*, Marcus A. Worsley, Theodore F. Baumann, Joe H. Satcher Jr.

Chem. Mater. **2010**, *13*, XXXX

Synthesis of ZnO coated Activated Carbon Aerogel by Simple Sol-Gel Route

A composite material of nanocrystalline ZnO coated activated carbon aerogel with high surface area is prepared by simple sol-gel chemistry. The coverage of ZnO nanoparticles on the carbon framework of ACA is very uniform. Thermal removal of carbon produce ZnO replica structure mimicking the original ACA framework.

